A Step Too Far? Assessment of the Boroxide Ligand in Ring-Opening Polymerization

Sarah C. Cole, Martyn P. Coles,* and Peter B. Hitchcock

Department of Chemistry, University of Sussex, Falmer, Brighton BN1 9QJ, U.K.

Received July 1, 2004

Dimesityl borinic acid, $(mes)_2BOH$ [mes = 2,4,6-$Me_3C_6H_2$], has been employed as a source of boroxide ligand in lithium, zinc, and magnesium chemistry; for structural comparisons, the alkoxide ligand $[OCH(mes)_2]^-$ has also been used. The lithium compounds $[Li\{OB(mes)_2\}(L)_n]_2$ [**1a**, L = Et_2O, *n* = 1; **1b**, L = Py, *n* = 1; **1c**, L = MeCN, *n* = 2] have been structurally characterized, showing a common bimetallic core with bridging boroxide ligands that differ in the relative rotation of the "BC_2" unit about the Li_2O_2 metallacycle. The zinc compounds $[Zn\{OR\}Me]_2$ [**2**, R = $B(mes)_2$; **3**, R = $CH(mes)_2$] have been synthesized from the reaction of $ZnMe_2$ with the corresponding ROH species. As for the Li salts, **2** and **3** display a dimeric solid-state structure with μ-OR ligands. Reaction of the in situ generated lithium boroxide **1a** with $MgBr_2{\cdot}Et_2O$ afforded an unprecedented tetrametallic compound, $[Mg\{OB(mes)_2\}Br{\cdot}LiBr(OEt_2)_2]_2$ (**4**), in which the lithium bromide side product is retained in a tricyclic structure containing a "Li(μ-Br)$_2$Mg{μ-OB(mes)$_2$}Mg(μ-Br)$_2$Li" core. The magnesium alkyl compounds $[Mg\{OB(mes)_2\}R(THF)]_2$ [**5**, R = Me; **6**, R = Bu] were obtained from the reaction of the Li salt with the Grignard reagent, MgMeBr, and protonolysis of $MgBu_2$ with $(mes)_2BOH$, respectively. X-ray crystallography showed formation of a dimer in each case, where in **6** only the *n*-butyl group was observed in the solid state. Attempts at combining the boroxide ligand with the widely used β-diketiminate ligand, $[HC\{C(Me)NAr\}_2]^-$ (BDI), at a zinc center are discussed, and a brief study into the potential of selected zinc complexes to initiate the ring-opening polymerization of ϵ-caprolactone and *rac*-lactide is described.

1. Introduction

Alkoxide anions remain one of the most widely applied ligands, and the chemistry surrounding their metal complexes has grown steadily in the last fifty years.[1] The properties of these ligands are routinely altered through derivitization of the *O*-substituent, allowing the generation of different steric and electronic environments at metal centers. For instance, sterically demanding groups have been extensively used to restrict the aggregation of metal alkoxides to molecular species in contrast to cluster systems by disfavoring bridging through the oxygen. Substituted phenyl frameworks, affording aryloxide compounds, are often used in this context,[2] where the availability of a large number of substituted phenols as precursors ensures access to a wide number of variants.

In addition to varying the steric properties of alkoxide ligands, it is possible to exercise control over the electronic properties, which may have a profound effect on the reactivity of the metal center. For example, it was demonstrated at an early stage in the development of the "Schrock" alkylidene metathesis catalysts, Mo(NAr)(CHR)(OR′)$_2$, that employing electron-poor fluoroalkoxide ligands markedly increased the reactivity toward certain substrates.[3] In the area of ring-opening metathesis polymerization (ROMP), it was shown that the tacticity of polymeric materials was also strongly influenced by which alkoxide group was used,[4] demonstrating that not only the reactivity but also the mechanism by which metals interact with substrates can be influenced by the supposedly innocent "ancillary" ligands.[5]

An alternative approach to exercising control of the donor properties of alkoxide-type ligands that circumvents the use of (often expensive) fluorinated alcohols is to incorporate an element that has π-acceptor properties adjacent to oxygen atom. Siloxide $[OSiR_3]^-$ and the boroxide $[OBR_2]^-$ ligands fit this criteria, where in the latter class, the empty p-orbital on the boron is able to accept electron density from the oxygen lone pairs, affording an "electron-poor" alkoxide. Work with this system was pioneered by Power and co-workers, in which it was demonstrated that the boroxides $[OBR_2]^-$ (R = mes = 2,4,6-$Me_3C_6H_2$; 2,4,6-$^iPr_3C_6H_2$) coordinated to group 8 and 9 metals in either a bridging or terminal coordination mode.[6] More recently this ligand has been used in main group systems,[7] and a recent structural report of the dimeric zinc compound $[Zn\{OB(mes)_2\}Et]_2$ has been presented.[8]

* To whom correspondence should be addressed. Fax: 01273 677196. Tel: 01273 877339. E-mail: m.p.coles@sussex.ac.uk.

(1) Bradley, D. C.; Mehrotra, R. C.; Gaur, D. P. *Metal Alkoxides*; Academic: New York, 1978. Mehrotra, R. C. *Adv. Inorg. Chem.* **1983**, *26*, 269.

(2) Rothwell, I. P. *Acc. Chem. Res.* **1988**, *21*, 153.

(3) Freudenberger, J.; Schrock, R. R.; Churchill, M.; Rheingold, A.; Ziller, J. *Organometallics* **1984**, *3*, 1563. Schrock, R. R. *Polyhedron* **1995**, *14*, 3177.

(4) Feast, W. J.; Gibson, V. C.; Marshall, E. L. *J. Chem. Soc., Chem. Commun.* **1992**, 1157.

(5) Schrock, R. R. *Tetrahedron* **1999**, *55*, 8141.

(6) Olmstead, M. M.; Power, P. P.; Sigel, G. *Inorg. Chem.* **1986**, *25*, 1027. Chen, H.; Power, P. P.; Shoner, S. C. *Inorg. Chem.* **1991**, *30*, 2884.

10.1021/om049520j CCC: $27.50
Publication on Web 09/25/2004

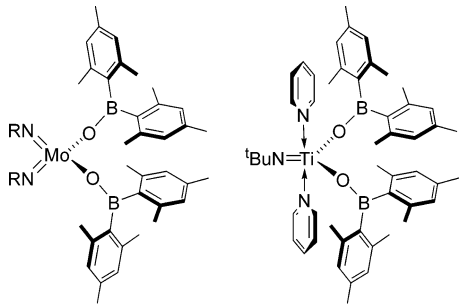

Figure 1.

Work in our group has attempted to show that the effect of the boron atom is real in both the solid state and solution, using a series of d^0-early transition metal imido compounds (Figure 1).[9] Crystallographic analysis showed a trend for the lengthening of the metal−oxygen bond in boroxide compounds, compared to the sterically similar $[OCH(mes)_2]^-$ alkoxide, and solution-state measurements of the $\Delta\delta$ value[10] for $Mo(N^tBu)_2\{OB(mes)_2\}_2$ and $Ti(N^tBu)\{OB(mes)_2\}_2(Py)_2$ were in agreement, supporting the idea that boroxide ligands behave as electron-deficient alkoxides.

There has been a recent surge in metal-alkoxide chemistry fueled by the application of certain compounds as well-defined initiators for ring-opening polymerization (ROP) of cyclic monomers.[11] In these instances, the M−OR linkage provides the active site for initiation via a coordination−insertion pathway, and much of the work has focused therefore on the development of suitable ancillary ligands that support this moiety during the course of the polymerization. To date, relatively nontoxic and cheap metals including aluminum, zinc, and magnesium have received the most attention in this area, although more "exotic" metals including lanthanum,[12] neodymium, and gadolinium[13] have also been investigated, demonstrating that this type of chemical reactivity may be promoted by many elements. As new systems are developed, the reactivity of the metal-alkoxide unit will need to be addressed, where, for example, a balance between adequate bulk that deters cluster formation while maintaining an active site that initiates ROP is required. We were therefore interested in studying the potential for the boroxide ligand to be applied in this context, given that evidence from our earlier studies indicates the electron-donating ability is similar to the aryloxide, which often suffers from poor initiation due to the bulk. However, the incorporation of the boron atom in boroxides has the advantage of removing the steric bulk from the vicinity of the metal, hopefully generating a site whereby polymerization will initiate. We report here a series of lithium, zinc, and magnesium complexes incorporating the dimesitylboroxide ligand, $[OB(mes)_2]^-$. Structural analyses have been performed to further our understanding of the way in which this anion interacts with metals, and a preliminary assessment of the potential for this ligand to initiate ROP of lactide is described.

2. Experimental Section

General Experimental Procedures. All manipulations were carried out under dry nitrogen using standard Schlenk and cannula techniques, or in a conventional nitrogen-filled glovebox. Solvents were dried over appropriate drying agent and degassed prior to use. The compounds $(mes)_2BOH$,[14] $(mes)_2CHOH$,[15] $MgMe_2$,[16] $H_2C\{C(Me)NAr\}_2H(BDI)H$,[17] Zn(BDI)Me,[18] and Zn(BDI)Et[19] were synthesized according to literature procedures. ^{n}BuLi (2.5 M solution in hexanes, Acros), $ZnMe_2$ (~2 M solution in toluene, Fluka), $MgBr_2{\cdot}Et_2O$ (Aldrich), and MgMeCl (3.0 M solution in THF, Aldrich) were purchased from the indicated sources and used as received. $MgBu_2$ was purchased as a 1.0 M solution in heptane from Aldrich. The volatiles were removed under vacuum, and the residue was redissolved in THF prior to use.

NMR spectra were recorded using a Bruker Avance DPX 300 MHz spectrometer at 300 (^{1}H) and 75 ($^{13}C\{^1H\}$) MHz. Proton and carbon chemical shifts are internally referenced to deuterated solvent and reported relative to TMS; coupling constants, *J*, are quoted in Hz. Elemental analyses were performed by S. Boyer at London Metropolitan University.

General Procedure for Synthesis of the Li Salts, 1a, 1b, and 1c. A solution of $(mes)_2BOH$ (0.50 g, 1.88 mmol) in ca. 35 mL of THF was cooled to 0 °C, and ^{n}BuLi (0.75 mL of a 2.5 M solution in hexanes, 1.88 mmol) was added. The mixture was allowed to warm to room temperature and stirred for 1 h, after which time clear dark yellow solutions were observed. The volatile components were removed in vacuo, and the residue was dissolved in the relevant solvent and stored at room temperature (**1a** and **1c**) or 4 °C (**1b**), affording colorless crystals of the solvated lithium boroxide. Accurate elemental analyses proved difficult to obtain in the case of **1b** and **1c**.

$[Li\{OB(mes)_2\}(Et_2O)]_2$ (1a). Anal. Calc for $C_{44}H_{64}B_2O_4Li_2$ (*692.49*): C, 76.32; H, 9.32. Found: C, 76.00; H, 9.51. ^{1}H NMR (C_6D_6, 298 K): δ 6.64 (s, 4H, C_6H_2), 3.13 (q, 4H, CH_2), 2.15 (s, 6H, 4-*Me*), 2.09 (s, 12H, 2,6-Me_2), 1.02 (t, 6H, CH_3). ^{13}C NMR (C_6D_6, 298 K): δ 143.0 (br, *C*), 138.9 (*C*H), 136.9 (*C*), 128.9 (*C*), 65.8 (CH_2, Et_2O), 22.2 (CH_3), 21.2 (CH_3), 15.3 (CH_3, Et_2O).

$[Li\{OB(mes)_2\}(Py)]_2$ (1b). ^{1}H NMR (C_6D_6, 298 K): δ 8.11 (m, 2H, *Py*), 6.89 (m, 1H, *Py*), 6.85 (s, 4H, C_6H_2), 6.55 (m, 2H, *Py*), 2.58 (s, 12H, 2,6-Me_2), 2.24 (s, 6H, 4-*Me*). ^{13}C NMR (C_6D_6, 298 K): δ 150.1 (*C*H, Py), 145.8 (br, *C*), 140.4 (*C*), 135.9 (*C*H, Py), 135.6 (*C*), 128.4 (*C*H), 123.4 (*C*H, Py), 22.9 (CH_3), 21.2 (CH_3).

$[Li\{OB(mes)_2\}(MeCN)_2]_2$ (1c). ^{1}H NMR (C_6D_6, 298 K): δ 6.70 (s, 4H, C_6H_2), 2.32 (s, 12H, 2,6-Me_2) 2.17 (s, 6H, 4-*Me*), −0.54 (s, 6H, *Me*CN). ^{13}C NMR (C_6D_6, 298 K): δ 143.7 (br, *C*),

(7) Gibson, V. C.; Mastroianni, S.; White, A. J. P.; Williams, D. J. *Inorg. Chem.* **2001**, *40*, 826. Anulewicz-Ostrowska, R.; Lulinski, S.; Serwatowski, J.; Suwinska, K. *Inorg. Chem.* **2000**, *39*, 5763.

(8) Anulewicz-Ostrowska, R.; Lulinski, S.; Pindelska, E.; Serwatowski, J. *Inorg. Chem.* **2002**, *41*, 2525.

(9) Cole, S. C.; Coles, M. P.; Hitchcock, P. B. *J. Chem. Soc., Dalton Trans.* **2002**, 4168.

(10) Nugent, W. A.; McKinney, R. J.; Kasowski, R. V.; van-Catledge, F. A. *Inorg. Chim. Acta* **1982**, *65*, L91.

(11) Darensbourg, D. J.; HoltcampM. W. *Coord. Chem. Rev.* **1996**, *153*, 155. O'Keefe, B. J.; Hillmyer, M. A.; Tolman, W. B. *J. Chem. Soc., Dalton Trans.* **2001**, 2215. Coates, G. W. *J. Chem. Soc., Dalton Trans.* **2002**, 467.

(12) Giesbrecht, G. R.; Whitener, G. D.; Arnold, J. *Dalton Trans.* **2001**, 923.

(13) Luo, Y.; Yao, Y.; Shen, Q.; Sun, J.; Weng, L. *J. Organomet. Chem.* **2002**, *662*, 144.

(14) Brown, H. C.; Dodson, V. H. *J. Am. Chem. Soc.* **1957**, *79*, 2302.

(15) Grilli, S.; Lunazzi, L.; Mazzanti, A.; Casarini, D.; Femoni, C. *J. Org. Chem.* **2001**, *66*, 488.

(16) Bailey, P. J.; Dick, C. M. E.; Fabre, S.; Parsons, S. *J. Chem. Soc., Dalton Trans.* **2000**, 1655.

(17) Stender, M.; Wright, R. J.; Eichler, B. E.; Prust, J.; Olmstead, M. M.; Roesky, H. W.; Power, P. P. *J. Chem. Soc., Dalton Trans.* **2001**, 3465. Feldman, J.; McLain, S. J.; Parthasarathy, A.; Marshall, W. J.; Calabrese, J. C.; Arthur, S. D. *Organometallics* **1997**, *16*, 1514.

(18) Prust, J.; Stasch, A.; Zheng, W.; Roesky, H. W.; Alexpoulos, E.; Uson, I.; Bohler, D.; Schuchardt, T. *Organometallics* **2001**, *20*, 3825.

(19) Cheng, M.; Moore, D. R.; Reczek, J. J.; Chamberlain, B. M.; Lobkovsky, E. B.; Coates, G. W. *J. Am. Chem. Soc.* **2001**, *123*, 8738.

140.1 (*C*H), 136.1 (*C*), 127.9 (*C*), 116.0 (CH_3CN), 22.8 (CH_3), 21.2 (CH_3), 1.4 (CH_3CN).

[Zn{OB(mes)$_2$}Me]$_2$ (2). A solution of $(mes)_2BOH$ (0.750 g, 2.82 mmol) in toluene (20 mL) was added dropwise at room temperature to a stirred solution of $ZnMe_2$ (1.41 mL of 2 M solution in toluene, 2.82 mmol, further diluted with an additional 20 mL of toluene), to afford a colorless solution and a white precipitate. After stirring for 14 h under ambient conditions the volatiles were removed under reduced pressure, and the resultant white solid was extracted by filtration from a small amount of insoluble material using toluene. Concentration and storage at 4 °C yielded **2** as colorless crystals. Yield: 0.914 g (94%). Anal. Calc for $C_{45}H_{58}B_2O_2Zn_2$ (*783.35*)†: C, 69.00; H, 7.46. Found: C, 68.30; H, 7.62. ^{1}H NMR (C_6D_6, 298 K): δ 6.73 (s, 4H, C_6H_2), 2.35 (s, 12H, 2,6-*Me*$_2$), 2.10 (s, 6H, 4-*Me*), −0.87 (s, 3H, Zn*Me*). ^{13}C NMR (C_6D_6, 298 K): δ 140.1 (br, *C*), 138.4 (*C*H), 128.8 (*C*), 127.7 (*C*), 23.0 (CH_3), 21.4 (CH_3), −15.1 (ZnCH_3) (†calculated for the mono-toluene solvate).

[Zn{OCH(mes)$_2$}Me]$_2$ (3). Compound **3** was prepared using the general procedure outlined for **2**, using 0.350 g of $(mes)_2CHOH$ (1.30 mmol) and 0.65 mL of a 2 M solution of $ZnMe_2$ in toluene (1.30 mmol). Concentration and storage at room temperature yielded **3** as opaque white crystals. Yield: 0.378 g (42%). Anal. Calc for $C_{40}H_{52}O_2Zn_2$ (*695.61*): C, 69.07; H, 7.53. Found: C, 69.10; H, 7.61. ^{1}H NMR (C_6D_6, 298 K): δ 6.70 (s, 4H, C_6H_2), 6.65 (s, 1H, C*H*), 2.28 (s, 12H, 2,6-*Me*$_2$) 2.08 (s, 6H, 4-*Me*), −0.75 (s, 3H, Zn*Me*). ^{13}C NMR (C_6D_6, 298 K): δ 139.2 (br, *C*), 136.3 (*C*), 135.9 (*C*), 131.3 (*C*H), 78.0 (*C*H), 21.9 (CH_3), 20.7 (CH_3), −16.9 (ZnCH_3).

[Mg{OB(mes)$_2$}Br·LiBr(Et$_2$O)$_2$]$_2$ (4). ^{n}BuLi (0.61 mL of a 2.5 M solution in hexanes, 1.58 mmol) was added dropwise to a cooled (0 °C) solution of $(mes)_2BOH$ (0.400 g, 1.50 mmol) in Et_2O (25 mL). The mixture was allowed to warm to room temperature and stirred for 45 min, affording a fine white precipitate of **1a**. The slurried lithium salt was added to a solution of $MgBr_2{\cdot}Et_2O$ (0.387 g, 1.50 mmol) in Et_2O (25 mL) and the resultant mixture stirred for 14 h at room temperature. Removal of the volatiles afforded a white solid that was extracted from a small amount of insoluble material with Et_2O. Concentration and storage at −30 °C yielded pure **4** as colorless crystals. Yield: 0.812 g (60%). Anal. Calc for $C_{36}H_{44}B_2Br_4Li_2Mg_2O_2$ (*912.47*)‡: C, 47.39; H, 4.86. Found: C, 47.49; H, 4.81 (‡formula corresponds to the desolvated complex, Mg{OB(mes)$_2$}Br·LiBr).

[Mg{OB(mes)$_2$}Me(THF)]$_2$ (5). ^{n}BuLi (0.61 mL of a 2.5 M solution in hexanes, 1.58 mmol) was added dropwise to a cooled (0 °C) solution of $(mes)_2BOH$ (0.400 g, 1.50 mmol) in Et_2O (25 mL). The mixture was allowed to warm to room temperature and stirred for 45 min, affording a fine white precipitate of **1a**. The slurried lithium salt was added to a cooled (−78 °C) solution of MgMeCl (0.50 mL of a 3 M solution in THF, 1.50 mmol, further diluted by addition of 20 mL of Et_2O). After stirring for 14 h under ambient conditions the volatiles were removed under reduced pressure, affording a white solid. Compound **5** was extracted from the lithium chloride side product with hot toluene (100 °C). Concentration and storage at 4 °C yielded **5** as colorless crystals. Yield: 0.167 g (30%). ^{1}H NMR (CD_2Cl_2, 298 K): δ 6.70 (s, 4H, C_6H_2), 3.32 (br m, 4H, *THF*), 2.29 (s, 12H, 2,6-*Me*$_2$), 2.20 (s, 6H, 4-*Me*), 1.62 (br m, 4H, *THF*), −1.86 (s, 3H, CH_3). ^{13}C NMR (CD_2Cl_2, 298 K): 141.6 (br, *C*), 140.4 (*C*), 137.4 (*C*), 128.2 (*C*H), 69.3 (CH_2, *THF*), 25.4 (CH_2, *THF*), 23.0 (CH_3), 21.1 (CH_3), −14.4 (MgCH_3).

[Mg{OB(mes)$_2$}^{n}Bu(THF)]$_2$ (6). A solution of $(mes)_2BOH$ (0.400 g, 1.50 mmol) in THF (20 mL) was added dropwise to a stirred solution of $MgBu_2{\cdot}THF$ (1.50 mL of a 1.0 M solution in THF, 1.50 mmol, further diluted with an additional 20 mL of THF) at −78 °C. The mixture was allowed to warm to room temperature and stirred for 14 h. Removal of the volatiles afforded a sticky white solid that was extracted from a small amount of insoluble white material with hexane. Concentration and storage at −30 °C afforded **6** as colorless crystals. Yield: 0.320 g, (25%). Anal. Calc for $C_{52}H_{78}B_2Mg_2O_4$ (*837.41*): C, 74.59; H, 9.39. Found: C, 69.05; H, 9.06. ^{1}H NMR (C_6D_6, 298 K): δ 6.76 (s, 4H, C_6H_2), 3.24 (br m, 4H, *THF*), 2.58 (s, 12H, 2,6-*Me*$_2$), 2.14 (s, 6H, 4-*Me*), 1.60 (m, 2H, CH_2), 1.44 (m, 2H, CH_2), 1.17 (t, J = 7.2, 3H, CH_3), 1.04 (br m, 4H, *THF*), −0.20 (m, 2H, MgCH_2). ^{13}C NMR (C_6D_6, 298 K): δ 141.9 (br, *C*), 140.6 (*C*), 137.3 (*C*), 128.6 (*C*H), 69.2 (CH_2, THF), 33.0 (CH_2), 32.8 (CH_2), 25.0 (CH_3), 23.4 (CH_3), 21.2 (CH_2, THF), 14.6 (CH_3), 9.8 (MgCH_2).

Crystallography. Details of the crystal data, intensity collection, and refinement for complexes **1a** and **1c** are listed in Table 1, for compounds **2** and **3** in Table 3, and for compounds **4**, **5**, and **6** in Table 5. Crystals were covered in oil, and suitable single crystals were selected under a microscope and mounted on a Kappa CCD diffractometer. The structures were refined with SHELXL-97.[20] Additional features are described below.

[Li{OB(mes)$_2$}(Et$_2$O)]$_2$ (1a). The crystals diffracted only very weakly. The molecule has a center of inversion.

[Li{OB(mes)$_2$}(MeCN)$_2$]$_2$ (1c). The molecule lies on a 2-fold rotation axis.

[Zn{μ-OB(mes)$_2$}Me]$_2$ (2). The molecule lies on a crystallographic mirror plane. The toluene solvate molecule was unresolved and was modeled only by including four peaks as carbon atoms at half occupancy, close to a mirror plane. The large values for the largest diffraction peak and hole (0.95 and −0.42 e Å^3, respectively) were located near the disordered solvate.

[Zn{μ-OCH(mes)$_2$}Me]$_2$ (3). The molecule has a center of inversion.

[Mg{OB(mes)$_2$}Br·LiBr(OEt$_2$)$_2$]$_2$ (4). Two independent molecules were present in the unit cell. Two of the Et_2O ligands showed partial disorder and were included with isotropic O and C atoms and SADI bond length constraints.

[Mg{OB(mes)$_2$}Me(THF)]$_2$ (5). The molecule has a center of inversion.

[Mg{OB(mes)$_2$}^{n}Bu(THF)]$_2$ (6). The molecule has a center of inversion.

3. Results and Discussion

3.1. Lithium Boroxide Compounds. Synthesis of metal boroxide compounds employing a borinic acid as the ligand precursor has been achieved using two general synthetic protocols. Protonolysis of a metal−carbon bond with the parent acids, R_2BOH, provides a clean route to the target species due to the volatile hydrocarbon side products, while transmetalation employing the lithiated reagent, $[Li\{OBR_2\}(solvent)_x]_n$, is a valuable approach due to the large number of metal-halide starting materials. Work in our group toward establishing the influence that boron exerts on the bonding parameters in titanium and molybdenum boroxide complexes[9] successfully utilized the latter approach, employing the imido complexes $Mo(NR)_2Cl_2(DME)$[21] and $Ti(NR)Cl_2(Py)_3$[22] as starting reagents. In these instances, synthesis of the compounds $Mo(NR)_2\{OB(mes)_2\}_2$ and $Ti(NR)\{OB(mes)_2\}_2(Py)_2$ proved most convenient using lithiated reagents that were generated in situ, although in previous studies in other groups, $[LiOB\{CH(SiMe_3)_2\}_2]_2$,[23] $[Li\{OB(mes)_2\}(THF)]_2$,[24] and

(20) Sheldrick, G. M. *SHELXL-97, Program for the Refinement of Crystal Structures*; Göttingen, 1997.
(21) Bell, A.; Clegg, W.; Dyer, P. W.; Elsegood, M. R. J.; Gibson, V. C.; Marshall, E. L. *J. Chem. Soc., Chem. Commun.* **1994**, 2547.
(22) Blake, A. J.; Collier, P. E.; Dunn, S. C.; Li, W.-S.; Mountford, P.; Shishkin, O. V. *J. Chem. Soc., Dalton Trans.* **1997**, 1549.

Scheme 1

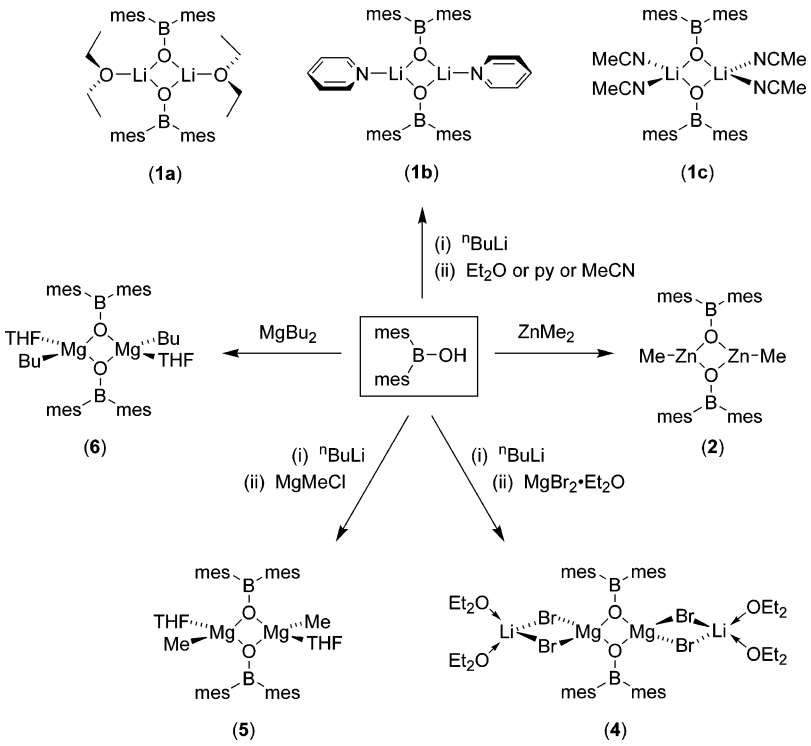

$[Li\{OB(fmes)_2\}(THF)]_2$[25] (fmes = 2,4,6-$(CF_3)_3C_6H_2$) have been isolated and structurally characterized.

During the course of our work a further three examples of lithium boroxide complexes, $[Li\{OB(mes)_2\}(Et_2O)]_2$, **1a**, $[Li\{OB(mes)_2\}(Py)]_2$, **1b**, and $[Li\{OB(mes)_2\}(MeCN)_2]_2$, **1c**, were isolated and structurally characterized (Scheme 1). Significant differences are evident in the molecular structures, dependent on the coordinated solvent, warranting a brief discussion. The molecular structures of **1a** and **1c** are illustrated in Figures 2 and 3, crystal data are summarized in Table 1, and selected bond lengths and angles are given in Table 2. A poor quality data set for the pyridine adduct, **1b**, was of insufficient accuracy to allow meaningful discussion of bond lengths and angles. It did however confirm the molecular structure as consisting of the dimeric monoadduct, $[Li\{OB(mes)_2\}(Py)]_2$.

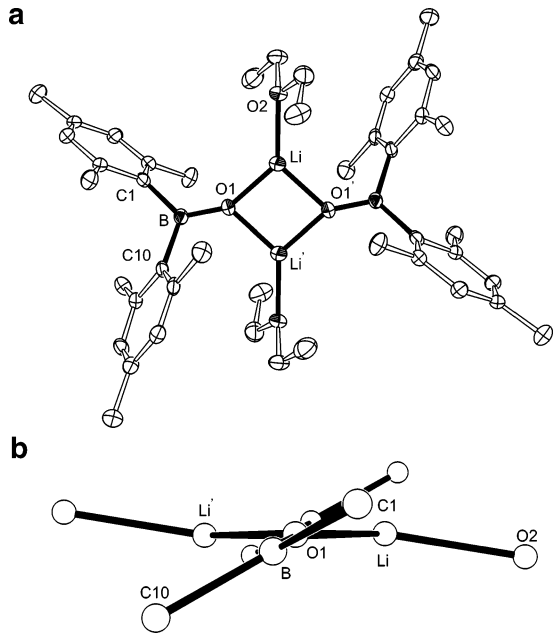

Figure 2. (a) Molecular structure of **1a** (thermal ellipsoids 30%; ′:$-x$, $-y$, $-z$). (b) Core of **1a** viewed along the transannular O····O vector of the Li_2O_2 metallacycle.

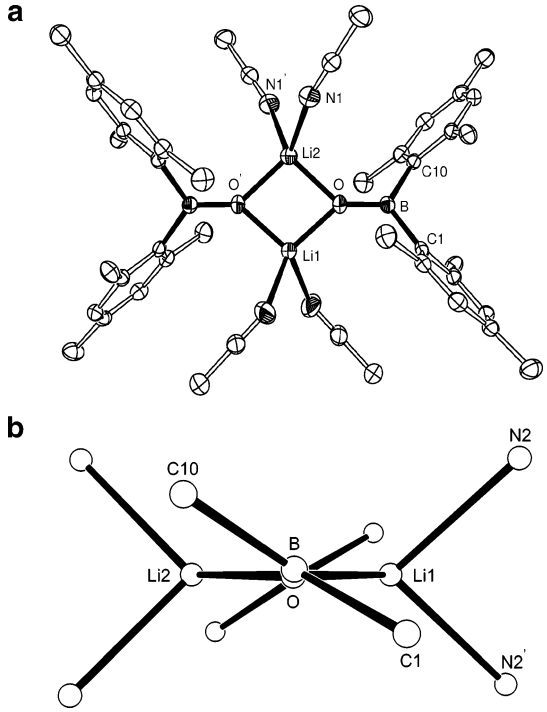

Figure 3. (a) Molecular structure of **1c** (thermal ellipsoids 30%; ′:$-x$, y, $-z+1/2$). (b) Core of **1c** viewed along the transannular O····O vector of the Li_2O_2 metallacycle.

As in previously reported structures of this general type, lithium salts **1a**−**c** consist of dimeric molecules

Table 1. Crystal Structure and Refinement Data for [Li{OB(mes)$_2$}(Et$_2$O)]$_2$ (1a) and [Li{OB(mes)$_2$}(MeCN)$_2$]$_2$ (1c)

	1a[a]	**1c**
formula	$C_{44}H_{64}B_2Li_2O_4$	$C_{44}H_{56}B_2Li_2N_4O_2$
fw	692.45	708.43
temperature (K)	173(2)	173(2)
wavelength (Å)	0.71073	0.71073
cryst size (mm)	0.10 × 0.05 × 0.01	0.30 × 0.30 × 0.20
cryst syst	monoclinic	monoclinic
space group	$P2_1/n$ (No.14)	$C2/c$ (No.15)
a (Å)	9.0303(4)	27.7092(13)
b (Å)	9.1269(4)	9.4616(6)
c (Å)	25.4398(11)	16.3004(7)
β (deg)	91.214(2)	91.119(3)
V (Å^3)	2096.2(2)	4272.7(4)
Z	2	4
D_{calc} (Mg/m^3)	1.10	1.10
absorp coeff (mm^{-1})	0.07	0.07
θ range for data collection (deg)	3.91 to 22.98	3.82 to 25.04
no. of reflns collected	11 272	10 157
no. of indep reflns	2766 [R_{int} = 0.129]	3764 [R_{int} = 0.058]
no. of reflns with $I>2\sigma(I)$	1871	2616
no. of data/restraints/params	2766/0/239	3764/0/275
goodness-of-fit on F^2	1.157	1.049
final R indices [$I>2\sigma(I)$]	R1 = 0.090	R1 = 0.056
	wR_2 = 0.191	wR_2 = 0.139
R indices (all data)	R_1 = 0.135	R_1 = 0.086
	wR_2 = 0.212	wR_2 = 0.157
largest diff peak and hole (e Å^{-3})	0.28 and −0.23	0.22 and −0.18

[a] Very weak diffraction.

Table 2. Selected Bond Lengths (Å) and Angles (deg) for [Li{OB(mes)$_2$}(Et$_2$O)]$_2$ (1a) and [Li{OB(mes)$_2$}(MeCN)$_2$]$_2$ (1b)

	1a	**1b**
B−O	1.331(6)	1.315(3)
Li−O[a]	1.827(8)	1.860(4)
Li−O[b]	1.889(9)	1.892(4)
O−Li−O	96.5(4)	97.4(3)[c] 95.2(3)[d]
Li−O−Li	83.5(4)	83.66(19)

[a] **1a** Li−O(1), **1b** Li(1)−O. [b] **1a** Li−O(1′), **1b** Li(2)−O. [c] O−Li(1)−O′. [d] O−Li(2)−O′.

containing a bimetallic Li_2O_2 core, with bridging boroxide ligands. The coordination sphere at lithium is completed by solvent in each case where, due to the smaller size and "rodlike" shape of acetonitrile, two molecules are accommodated in **1c**, affording distorted tetrahedral centers. In contrast, a single solvate is present in **1a** and **1b**, generating a distorted trigonal planar lithium with slight pyramidalization [Σ_{angles} = 358.5°] for the Et$_2$O adduct. **1c** therefore extends this series of compounds of general formula [Li{μ-OBR$_2$}(solvent)$_x$]$_2$, from x = 0 [R = CH(SiMe$_3$)$_2$][23] and x = 1 [R = mes; solvent = THF,[24] Et$_2$O (**1a**), Py (**1b**)] to x = 2 [R = mes; solvent = MeCN (**1c**)].

The Li_2O_2 metallacycles of **1a** and **1c** are both planar, with the major structural difference being the way in which the mesityl substituents are positioned in the solid state, a consequence of the different symmetry elements (i.e., **1a** has a center of inversion; **1c** lies on a 2-fold rotation axis). Therefore in **1a**, each −B(mes)$_2$ group is effectively rotated in an opposite direction along the B−O bond, with respect to the Li_2O_2 plane, while in **1c**, both groups are rotated in the same direction. Another consequence of locating the solvate in the Li_2O_2 plane within **1a** is a large distortion from ideal trigonal planar geometry at the oxygen atom [Li−O(1)−B, 148.6(4)°; Li′−O(1)−B, 126.3(4)°], whereas equivalent angles are observed in **1c**. The corresponding Li−O bond distances are essentially identical for **1a** and **1c** (within esd's), although notable asymmetry is present within the boroxide bridge in **1a** [Li−O(1) = 1.827(8) Å; Li−O(2) = 1.889(9) Å].

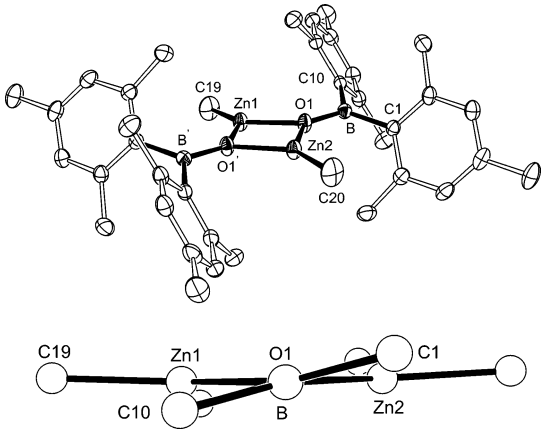

Figure 4. Molecular structure of **2** (thermal ellipsoids 30%; ′: x, $-y$+3/2, z).

3.2. Zinc Boroxide Compounds. Initial studies toward the introduction of a boroxide ligand at a zinc center focused on the reaction of the in situ generated lithium salts, [Li{OB(mes)$_2$}(solvent)$_x$]$_n$, with zinc dibromide. Analysis of the crude product by ^{1}H NMR spectroscopy indicated three different environments for the mesityl groups, and no clean product could be isolated from the reaction. The protonolysis reaction between 1 equiv of (mes)$_2$BOH and ZnMe$_2$, however, proceeded cleanly at room temperature to afford colorless crystals of **2** in excellent yield (Scheme 1). NMR data and combustion analysis were consistent with formation of the desired mixed alkylzinc boroxide complex, [Zn{OB(mes)$_2$}Me]$_n$,[26] although no data concerning the extent of aggregation could be obtained by mass spectral analysis (EI$^+$), the highest molecular weight fragment observed corresponding to the ligand [OB(mes)$_2$]$^+$.

The molecular structure of **2** is illustrated in Figure 4, crystal data are summarized in Table 3, and selected bond lengths and angles are given in Table 4. Analogous to the zinc ethyl analogue,[8] compound **2** crystallizes as the dimeric complex [Zn{μ-OB(mes)$_2$}Me]$_2$. The zinc atom is distorted trigonal planar [Σ_{angles} = 359.96°], coordinated to two bridging boroxides and a terminal methyl group. The bridging coordination mode for the boroxide ligand is unremarkable[6,7,24] and may be favored in these systems by the presence of the boron, which

(23) Beck, G.; Hitchcock, P. B.; Lappert, M. F.; Mackinnon, I. A. *J. Chem. Soc., Chem. Commun.* **1989**, 1312.
(24) Weese, K. J.; Bartlett, R. A.; Murray, B. D.; Olmstead, M. M.; Power, P. P. *Inorg. Chem.* **1987**, *26*, 2409.
(25) Gibson, V. C.; Redshaw, C.; Clegg, W.; Elsegood, M. R. J. *Polyhedron* **1997**, *16*, 2637.
(26) Cole, S. C.; Coles, M. P.; Hitchcock, P. B. *Dalton Trans.* **2003**, 3663.

Table 3. Crystal Structure and Refinement Data for [Zn{OB(mes)$_2$}Me]$_2$ (2) and [Zn{OCH(mes)$_2$}Me]$_2$ (3)

	2	3
formula	$C_{38}H_{50}B_2O_2Zn_2.(C_7H_8)$	$C_{40}H_{52}O_2Zn_2$
fw	783.27	695.56
temperature (K)	173(2)	173(2)
wavelength (Å)	0.71073	0.71073
cryst size (mm)	0.2 × 0.2 × 0.2	0.2 × 0.2 × 0.1
cryst syst	orthorhombic	triclinic
space group	*Pnma* (No. 62)	$P\bar{1}$ (No. 2)
a (Å)	16.3684(2)	8.0099(1)
b (Å)	26.5187(5)	10.5839(2)
c (Å)	9.7433(2)	11.6288(2)
α (deg)	90	105.530(1)
β (deg)	90	108.855(1)
γ (deg)	90	93.507(1)
V (Å^3)	4229.3(1)	887.01(3)
Z	4	1
D_{calc} (Mg/m^3)	1.23	1.30
absorp coeff (mm^{-1})	1.17	1.38
θ range for data collection (deg)	3.92 to 25.22	3.80 to 25.05
no. of reflns collected	22824	9558
no. of indep reflns	3686 [R_{int} = 0.074]	3094 [R_{int} = 0.034]
no. of reflns with $I>2\sigma(I)$	2859	2862
no. of data/restraints/params	3686/0/227	3094/0/205
goodness-of-fit on F^2	1.055	0.575
final *R* indices [$I>2\sigma(I)$]	$R_1 = 0.056$, $wR_2 = 0.171$	$R_1 = 0.026$, $wR_2 = 0.070$
R indices (all data)	$R_1 = 0.075$, $wR_2 = 0.185$	$R_1 = 0.029$, $wR_2 = 0.074$
largest diff peak and hole (e Å^{-3})	0.95 and −0.42	0.25 and −0.37

Table 4. Selected Bond Lengths (Å) and Angles (deg) for [Zn{OB(mes)$_2$}Me]$_2$ (2) and [Zn{OCH(mes)$_2$}Me]$_2$ (3)

	2	3
Zn−O[a]	1.965(3)	1.954(1)
Zn−O[b]	1.970(3)	1.946(1)
Zn−C[c]	1.922(7)	1.938(2)
Zn(2)−C(20)	1.921(6)	
B−O	1.353(5)	
C(1)−O		1.423(2)
O−Zn−O[d]	81.26(15)	79.46(6)
O−Zn−O[e]	81.00(15)	
O−Zn−C[f]	139.35(8)	138.28(8)
O−Zn−C[g]	139.48(8)	142.22(8)
Zn−O−Zn[h]	98.85(12)	100.54(6)

[a] **2** Zn(1)−O(1), **3** Zn−O. [b] **2** Zn(2)−O(1), **3** Zn−O′. [c] **2** Zn(1)−C(19), **3** Zn−C(20). [d] **2** O(1)−Zn(1)−O(1′). [e] **2** O(1)−Zn(2)−O(1′). [f] **2** O(1)−Zn(1)−C(19), **3** O−Zn−C(20). [g] **2** O(1)−Zn(2)−C(20), **3** O′−Zn−C(20). [h] **2** Zn(1)−O(1)−Zn(2), **3** Zn−O−Zn′.

displaces the bulk of the mesityl groups from the anionic oxygen atom, allowing the interaction with two metal fragments.

The planarity of the metallacycle extends to include the boron atom and terminal methyl substituent (max. deviation from the plane = 0.09 Å) with a twist angle between the metallacycle and the plane defined by the −BC$_2$ fragment of 13.95(11)°. The internal angles at zinc and oxygen [81.26(15)°/81.00(15)° and 98.85(12)°, respectively] are similar to the corresponding angles in the zinc ethyl complex[8] and in the related dimeric alkoxides [Zn(*μ*-OAr)(CH$_2$SiMe$_3$)]$_2$ (Ar = 2,6-^{i}Pr$_2$C$_6$H$_3$ and 2,4,6-^{t}Bu$_3$C$_6$H$_2$).[27] The Zn−O bond lengths are equal within experimental error [1.965(3) and 1.970(3) Å], suggesting a strong association of the Zn{OB(mes)$_2$}-

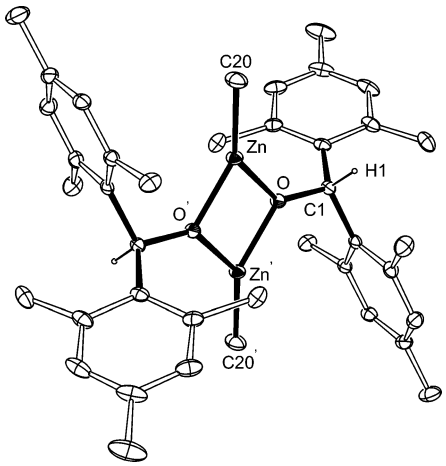

Figure 5. Molecular structure of **3** (thermal ellipsoids 30%; ′: −*x*+1, −*y*+1, −*z*+1).

Me units. In contrast, the related aryloxide [Zn(*μ*-Omes*)(CH$_2$SiMe$_3$)]$_2$ contains one long [2.021(4) Å] and one short [1.958(4) Å] Zn−O bond and may therefore be considered as consisting of a more loosely held dimer, presumably on account of the steric bulk at zinc.

To evaluate the electronic influence of the boron atom on the metal−oxygen bond in **2**, we investigated the protonolysis reaction between the alcohol, (mes)$_2$CHOH,[15] and ZnMe$_2$ (eq 1). We have previously described the use

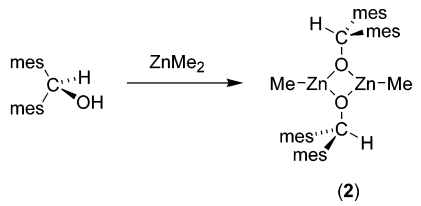

(1)

(2)

of this group as a system sterically comparable to dimesityl boroxide,[9] enabling a more representative investigation of the electronic influences of the B atom to be conducted. The reaction proceeded cleanly to afford colorless crystals of [Zn{OCH(mes)$_2$}Me]$_n$ (**3**). The key features of the ^{1}H NMR spectrum are the low-field shift of *δ* 6.65 observed for the C*H* of the alkoxide and the high-field Zn*Me* resonance, *δ* −0.75. The molecular structure is illustrated in Figure 5, crystal data are summarized in Table 3, and selected bond lengths and angles are given in Table 4.

Compound **3** is also dimeric in the solid state, with the molecular formula [Zn{*μ*-OCH(mes)$_2$}Me]$_2$. The Zn$_2$O$_2$ metallacycle is planar, consisting of distorted trigonal zinc and oxygen atoms, with the methyl carbon atom displaced from this plane by 0.16 Å. The uncertainty in the metal−oxygen bond distances for **2** and **3** precludes any definitive conclusions from being made regarding a possible reduction in bond order for the boroxide, although a more pronounced tendency toward inequivalent zinc−oxygen bonds [1.946(1) and 1.954(1) Å] is noted in **3**. The zinc−carbon distance [1.938(2) Å] is experimentally the same as the corresponding values in **2** [1.922(7) and 1.921(6) Å], again preventing any conclusions to be made concerning the effect of the boron atom.

(27) Olmstead, M. M.; Power, P. P.; Shoner, S. C. *J. Am. Chem. Soc.* **1991**, *113*, 3379.

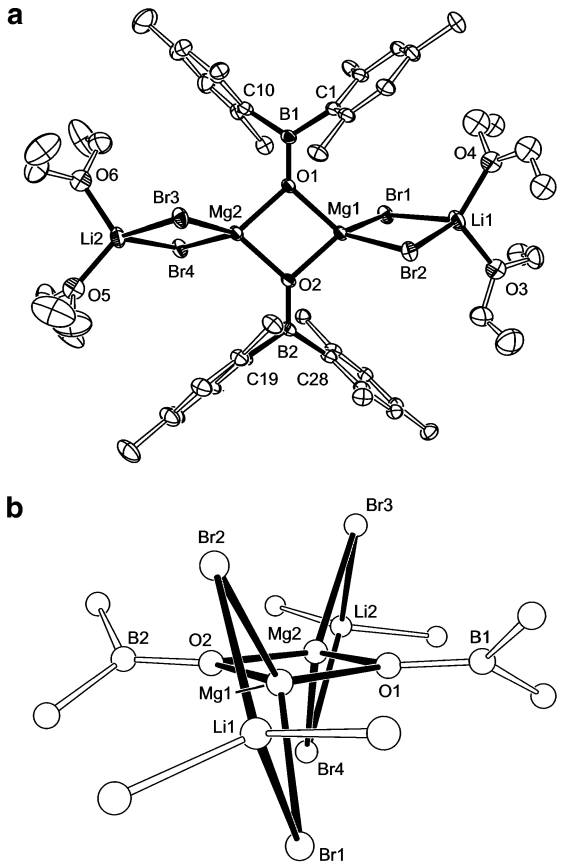

Figure 6. (a) Molecular structure of **4** (thermal ellipsoids 30%). (b) View of the tricyclic core of **4**.

3.3. Magnesium Boroxide Compounds. Magnesium is another metal of interest in the context of initiators for the ring-opening polymerization of cyclic esters.[28] Initial attempts at the synthesis of magnesium boroxide catalysts focused on a salt metathesis route employing $MgBr_2 \cdot Et_2O$ as the source of metal. Addition of a slurry of 1 equiv of the in situ generated salt $[Li\{OB(mes)_2\}(Et_2O)_x]_n$ (**1a**) to a cooled solution of $MgBr_2 \cdot Et_2O$ afforded the lithium magnesate $[Mg\{OB(mes)_2\}Br \cdot LiBr(Et_2O)_2]_n$ (**4**). The low solubility and apparent decomposition of **4** in a range of solvents precluded the collection of NMR data. However, combustion analysis on a sample that had been exposed to vacuum for 6 h was consistent with the desolvated species $Mg\{OB(mes)_2\}Br \cdot LiBr$, and crystals suitable for X-ray analysis were obtained from cooling a saturated Et_2O solution to −35 °C. The molecular structure is illustrated in Figure 6, crystal data are summarized in Table 5, and selected bond lengths and angles are given in Table 6. Two molecules are present in the unit cell with small differences in the bond lengths and angles; for brevity, values referring to only one molecule will be referred to in the discussion.

Compound **4** exists as the dimeric magnesate $[Mg\{OB(mes)_2\}Br \cdot LiBr(Et_2O)_2]_2$, containing the previously unreported tetrametallic $Li(\mu\text{-}X)_2Mg\{\mu\text{-}OR\}_2Mg(\mu\text{-}X)_2Li$ core [X = Br and R = B(mes)$_2$] formed of four tetrahedral metal centers bridged by pairs of bromine or oxygen atoms. The only other structurally characterized example containing this arrangement of metal atoms is the lithium−magnesium mixed amide species $[\{LiMg(TMP)[CH_2SiMe_2N(SiMe_3)]\}_2]$.[29] This structure is however fundamentally different, as the central component consists of a 5-fold system of fused four-membered rings rather than the three distinct metallacycles present in **4**. The geometry at magnesium is distorted tetrahedral, with bond angles in the range 83.83(16)−128.37(14)° and 84.08(16)−125.65(14)° for Mg(1) and Mg(2), respectively. The most acute angle at magnesium is within the central Mg_2O_2 metallacycle, which forms an essentially planar component (max. deviation from the plane = 0.015 Å). Large twist angles to the two $MgBr_2$-Li rings are noted [74.33° and 77.25° for Mg(1)−Br(1/2)−Li(1) and Mg(2)−Br(3/4)−Li(2) respectively], where these two units are rotated in opposite direction relative to each other (Figure 6b), presumably to minimize steric interactions. The Mg−O bond lengths within the core [1.96 Å av] are slightly contracted compared with the corresponding lengths in the related dimers $[Mg\{OB(mes)_2\}R(THF)]_2$ (R = Me, ^{n}Bu, vide infra).

Making use of readily available Grignard reagents, formation of the Mg−O linkage can be envisaged in two ways: transmetalation of the Mg−X bond with lithiated borinic acid to afford $[Mg\{OB(mes)_2\}R]_n$ and protonolysis of the Mg−C bond to give $[Mg\{OB(mes)_2\}X]_n$ (X = halide). The Grignard reagent, MgMeCl, was investigated as an alternative source of magnesium employing the transmetalation protocol where, if successful, the reaction would afford a potential catalyst, directly building on Chen's observation that methyl ligands behave as ancillary groups in Al complexes active for ROP.[30] The reaction afforded a colorless crystalline material, which from ^{1}H and ^{13}C NMR spectroscopic data was consistent with the monosolvated alkylmagnesium boroxide $[MgMe\{OB(mes)_2\}(THF)]_n$ (**5**). However, repeated attempts at obtaining accurate elemental analysis failed, due we believe to the high sensitivity of this class of compound and incomplete separation from the lithium chloride side product during workup. Structural analysis of a representative crystal, however, confirmed the product as the mono-THF adduct (vide infra).

Further difficulties associated with this methodology became apparent, as, despite numerous attempts, the synthesis of **5** could not be repeated using this protocol.[31] Despite being able to identify the product in the crude ^{1}H NMR spectrum on occasion, isolation of the pure compound was not successful due, we believe, to the high sensitivity of this synthetic approach to reaction conditions and the possible instability of the products. In addition, difficulties in purification via selective crystallization (due to the similar solubility properties of the magnesium compound and the lithium halide side products) resulted in low yields and inaccurate elemental analyses. Alternative methods for the introduction of the boroxide ligand at magnesium were therefore investigated.

(28) Chisholm, M. H.; Huffman, J. C.; Phomphrai, K. *J. Chem. Soc., Dalton Trans.* **2001**, 222.

(29) Barr, L.; Kennedy, A. R.; MacLellan, J. G.; Moir, J. H.; Mulvey, R. E.; Rodger, P. J. A. *J. Chem. Soc., Chem. Commun.* **2000**, 1757.

(30) Chakraborty, D.; Chen, E. Y. X. *Organometallics* **2002**, *21*, 1438.

(31) Variations in conditions and reagents that were investigated in an attempt to overcome these problems included the use of fresh batches of recrystallized ligand, isolation of the lithium salt rather than reacting the reagents in situ, changing the Grignard from the chloride to the bromide, and performing the reaction in THF or Et_2O.

Table 5. Crystal Structure and Refinement Data for [Mg{OB(mes)$_2$}Br·LiBr(OEt$_2$)$_2$]$_2$ (4) [Mg{OB(mes)$_2$}Me(THF)]$_2$ (5), and [Mg{OB(mes)$_2$}^{n}Bu(THF)]$_2$ (6)

	4	5	6
formula	$C_{52}H_{84}B_2Br_4Li_2Mg_2O_6$	$C_{46}H_{66}B_2Mg_2O_4$	$C_{52}H_{78}B_2Mg_2O_4$
fw	1208.95	753.23	837.38
temperature (K)	173(2)	173(2)	173(2)
wavelength (Å)	0.71073	0.71073	0.71073
cryst size (mm)	0.40 × 0.40 × 0.40	0.30 × 0.30 × 0.20	0.35 × 0.35 × 0.15
cryst syst	monoclinic	monoclinic	triclinic
space group	*P*2/*c* (No. 13)	*P*2$_1$/*n* (No. 14)	*P*$\bar{1}$ (No. 2)
a (Å)	23.7839(3)	14.9529(2)	10.2085(5)
b (Å)	16.7263(2)	10.4052(2)	11.3243(6)
c (Å)	32.1496(3)	15.4761(2)	12.9560(7)
α (deg)	90	90	111.292(2)
β (deg)	98.462(1)	114.518(1)	94.887(2)
γ (deg)	90	90	111.725(2)
V (Å^3)	12650.4(2)	2190.78(6)	1253.99(11)
Z	8	2	1
D_{calc} (Mg/m^3)	1.27	1.14	1.11
absorp coeff (mm^{-1})	2.61	0.10	0.09
θ range for data collection (deg)	3.71 to 25.70	3.74 to 25.03	3.70 to 25.64
no. of reflns collected	169 906	22 701	20 077
no. of indep reflns	23 430 [R_{int} = 0.097]	3839 [R_{int} = 0.048]	4585 [R_{int} = 0.063]
no. of reflns with $I>2\sigma(I)$	16 672	3283	3447
no. of data/restraints/params	23 430/56/1206	3839/0/249	4585/0/277
goodness-of-fit on F^2	0.950	1.032	1.044
final *R* indices [$I>2\sigma(I)$]	R_1 = 0.061, wR_2 = 0.163	R_1 = 0.050, wR_2 = 0.129	R_1 = 0.058, wR_2 = 0.125
R indices (all data)	R_1 = 0.095, wR_2 = 0.189	R_1 = 0.060, wR_2 = 0.136	R_1 = 0.087, wR_2 = 0.138
largest diff peak and hole (e Å^{-3})	0.69 and −0.68	0.40 and −0.51	0.22 and −0.23

Table 6. Selected Bond Lengths (Å) and Angles (deg) for [Mg{OB(mes)$_2$}Br·LiBr(OEt$_2$)$_2$]$_2$ (4)

Mg(1)−O(1)	1.966(4)	Mg(2)−O(1)	1.966(4)
Mg(1)−O(2)	1.969(4)	Mg(2)−O(2)	1.960(4)
Mg(1)−Br(1)	2.4776(18)	Mg(2)−Br(3)	2.4674(19)
Mg(1)−Br(2)	2.474(2)	Mg(2)−Br(4)	2.472(4)
Li(1)−Br(1)	2.552(13)	Li(2)−Br(3)	2.566(12)
Li(1)−Br(2)	2.576(11)	Li(2)−Br(4)	2.588(12)
B(1)−O(1)	1.357(7)	B(2)−O(2)	1.346(7)
O(1)−Mg(1)−O(2)	83.83(16)	O(1)−Mg(2)−O(2)	84.08(16)
O(1)−Mg(1)−Br(1)	108.80(13)	O(1)−Mg(2)−Br(3)	110.76(13)
O(1)−Mg(1)−Br(2)	128.37(14)	O(1)−Mg(2)−Br(4)	125.65(14)
O(2)−Mg(1)−Br(1)	127.40(14)	O(2)−Mg(2)−Br(3)	125.25(14)
O(2)−Mg(1)−Br(2)	110.95(14)	O(2)−Mg(2)−Br(4)	110.24(13)
Br(1)−Mg(1)−Br(2)	100.24(7)	Br(3)−Mg(2)−Br(4)	102.45(7)
O(1)−B(1)−C(1)	119.1(5)	O(2)−B(2)−C(19)	119.6(5)
O(1)−B(1)−C(10)	120.1(5)	O(2)−B(2)−C(28)	119.3(5)
C(1)−B(1)−C(10)	120.7(5)	C(19)−B(2)−C(28)	121.5(3)
Mg(1)−O(1)−B(1)	132.2(4)	Mg(1)−O(2)−B(2)	132.3(4)
Mg(2)−O(1)−B(1)	131.8(4)	Mg(2)−O(2)−B(2)	131.6(4)
Mg(1)−O(1)−Mg(2)	95.97(17)	Mg(1)−O(2)−Mg(2)	96.06(17)
Mg(1)−Br(1)−Li(1)	81.8(3)	Mg(2)−Br(3)−Li(2)	80.7(3)
Mg(1)−Br(2)−Li(1)	81.4(3)	Mg(2)−Br(4)−Li(2)	80.1(3)
Br(1)−Li(1)−Br(2)	95.6(4)	Br(3)−Li(2)−Br(4)	96.7(4)

The first attempt at developing an alternative method for the synthesis of Mg boroxide compounds was the reaction of (mes)$_2$BOH with MgMeCl, predicted to proceed via protonolysis to afford [Mg{OB(mes)$_2$}Cl]$_n$. The reaction resulted in formation of a highly insoluble white powder, which resisted all attempts at purification. The next approach employed $MgMe_2$ as the starting reagent, also predicted to react via protonolysis with (mes)$_2$BOH, in an alternative route to **5**. Initial reactions in toluene were hampered by poor solubility of both reagents and products, and in an attempt to resolve this, the THF adduct of $MgMe_2$ was employed.[16] In this case, pure **5** could be isolated in very low (∼5%) yield, demonstrating that this route is successful for the synthesis of magnesium boroxides, although the small amount of isolated material makes it impractical as a viable entry point to the study of this chemistry.

The final magnesium reagent used in this study was dibutylmagnesium, commercially available as the 1:1 mixture of *n*-butyl and *sec*-butyl species in heptane.[32] Initial protonolysis reactions using this solution were unsuccessful, and so in an attempt to overcome this, a 1.0 M THF solution was made.[33] One equivalent of (mes)$_2$BOH was added at room temperature and the crystallized product analyzed using spectroscopic and X-ray diffraction techniques. ^{1}H and ^{13}C NMR spectra were consistent with the formula [Mg{OB(mes)$_2$}Bu(THF)]$_n$, and the resonance at δ −0.20 in the proton NMR spectrum is attributable to the α-C*H*$_2$ of the *n*-butyl ligand, with no corresponding resonance in the region of ∼+0.2 ppm predicted for the *sec*-butyl isomer.[34] These data suggest that the ^{n}Bu isomer crystallizes preferentially over the ^{s}Bu one, subsequently confirmed by X-ray crystallography. This is in contrast to the related compound [Mg{OAr′}Bu]$_2$ (Ar′ = 2,6-^{t}Bu$_2$C$_6$H$_3$), where the molecular structure consists of the *sec*-butyl isomer.[35]

Early studies of the solution-state structures of alkylmagnesium alkoxides concluded that bulky alkoxides favor formation of solvated dimers, while smaller alkoxy groups form unsolvated aggregates containing between four and seven monomeric units.[36] Only a few examples of structurally characterized [Mg{OR}R′]$_n$ complexes have been reported, showing a number of different structural types. For example, dimeric aryloxide compounds [Mg{OAr″}(*n*-hex)]$_2$ (Ar″ = 2,6-^{t}Bu$_2$-4-MeC$_6$H$_2$)[37] and the aforementioned *sec*-butyl complex [Mg-

(32) Duff, A. W.; Hitchcock, P. B.; Lappert, M. F.; Taylor, R. G.; Segal, J. A. *J. Organomet. Chem.* **1985**, *293*, 271.
(33) Tenorio, M. J.; Puerta, M. C.; Salcedo, I.; Valerga, P. *J. Chem. Soc., Dalton Trans.* **2001**, 653.
(34) Dove, A. P.; Gibson, V. C.; Hormnirun, P.; Marshall, E. L.; Segal, J. A.; White, A. J. P.; Williams, D. J. *Dalton Trans.* **2003**, 3088.
(35) Henderson, K. W.; Honeyman, G. W.; Kennedy, A. R.; Mulvey, R. E.; Parkinson, J. A.; Sherrington, D. C. *Dalton Trans.* **2003**, 1365.
(36) Coates, G. E.; Ridley, D. *Chem. Commun.* **1966**, 560. Ashby, E. C.; Nackashi, J.; Parris, G. E. *J. Am. Chem. Soc.* **1975**, *97*, 3162.
(37) Gromada, J.; Mortreux, A.; Chenal, T.; Ziller, J. W.; Leising, F.; Carpentier, J. F. *Chem.-Eur. J.* **2002**, *8*, 3773.

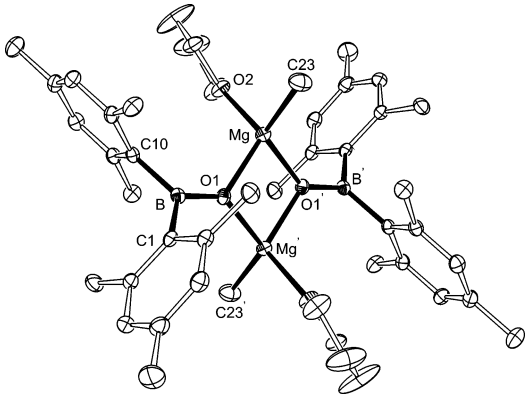

Figure 7. Molecular structure of **5** (thermal ellipsoids 30%; ′: $-x, -y, -z$).

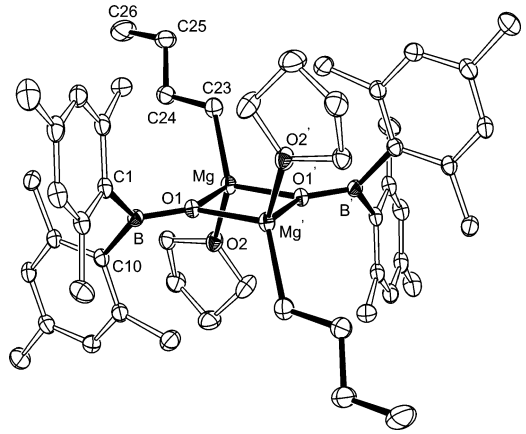

Figure 8. Molecular structure of **6** (thermal ellipsoids 30%; ′: $-x+2, -y+1, -z$).

{OAr′}Bu]$_2$ (Ar′ = 2,6-^{t}Bu$_2$C$_6$H$_3$) have been characterized, in which the steric bulk around the metal is sufficient to stabilize a three-coordinate magnesium, while reducing the steric volume in the *tert*-butoxy complex [Mg{O^{t}Bu}Me]$_4$ allows formation of a tetrameric cubane structure.[38] The molecular structures of **5** and **6** are illustrated in Figures 7 and 8, crystal data are summarized in Table 5, and selected bond lengths and angles are collected in Table 7.

Compounds **5** and **6** also exist as dimers in the solid state with bridging boroxide ligands and terminal alkyl groups. Displacement of the steric bulk of the mesityl substituents due to the inclusion of boron allows the coordination sphere of each magnesium to be completed by a molecule of THF, which form an *anti* arrangement with respect to the central Mg_2O_2 plane. The geometry at the metal center is therefore distorted tetrahedral, with bond angles in the range 84.31(6)−122.25(9)° for **5** and 84.77(7)−121.42(9)° for **6**, where, as noted in **4**, the smallest value angle corresponds to the internal angle within the metallacycle. The Mg−O bond lengths [**5**, 2.0077(15) and 1.9910(14) Å; **6** 2.005(2) and 2.006(2) Å] are on average longer than in the closely related bis-alkoxide and -siloxide complexes [Mg(OR)$_2$(THF)]$_2$ (R = CMePh$_2$; SiPh$_3$).[39] This is consistent with the proposed reduction of the metal−oxygen bond order arising from reduced π-component. However, in view of

Table 7. Selected Bond Lengths (Å) and Angles (deg) for [Mg{OB(mes)$_2$}Me(THF)]$_2$ (5) and [Mg{OB(mes)$_2$}^{n}Bu(THF)]$_2$ (6)

	5	6
Mg−O(1)	2.0077(15)	2.006(2)
Mg−O(1′)	1.9910(14)	2.005(2)
Mg−C(23)	2.117(2)	2.135(3)
Mg−O(2)	2.0342(15)	2.040(2)
B−O(1)	1.347(2)	1.356(3)
O(1)−Mg−O(1′)	84.31(6)	84.77(7)
O(2)−Mg−O(1′)	113.78(6)	112.79(7)
O(1)−Mg−O(2)	114.05(6)	109.04(7)
O(1)−Mg−C(23)	116.89(9)	121.42(9)
O(1′)−Mg−C(23)	122.25(9)	118.40(9)
O(2)−Mg−C(23)	105.07(9)	108.68(9)
O(1)−B−C(1)	118.66(7)	118.11(19)
O(1)−B−C(10)	118.93(17)	119.2(2)
C(1)−B−C(10)	122.40(16)	122.63(19)
Mg−O(1)−B	126.45(13)	129.66(14)
Mg′−O(1)−B	137.11(13)	134.81(14)
Mg−O(1)−Mg′	95.69(6)	95.23(7)

no additional metrical data to substantiate this idea (e.g., significant shortening of the Mg−C distance), lack of directly analogous compounds with which to compare bond lengths, and no method to examine the bonding in the solution state, we are cautious in claiming that the observed bonding patterns are solely due to the boron atom, and not at least partly due to differences in the steric environment at the metal center and/or crystal packing forces.

3.4. Attempted Synthesis of [Zn(BDI){OB(mes)$_2$}]$_n$ (BDI = [HC{C(Me)NAr}$_2$]$^-$). A large family of zinc-based ROP catalysts have been developed employing monoanionic β-diketiminate ligands [HC{C(Me)NAr}$_2$]$^-$ (BDI)[40] as a support for the metal alkoxide or amide bonds, which are the active component in this process.[11] To allow a more direct comparison to be made between existing catalysts and postulated systems based on the boroxide ligand, we targeted compounds of general formula [Zn(BDI){OB(mes)$_2$}]$_n$ using two different synthetic approaches (eqs 2a−c).

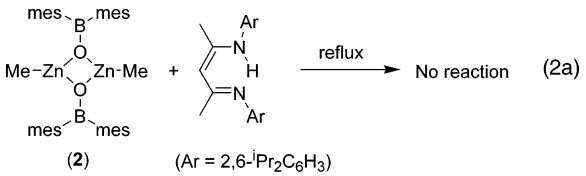

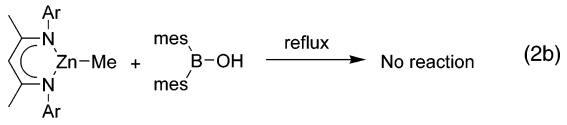

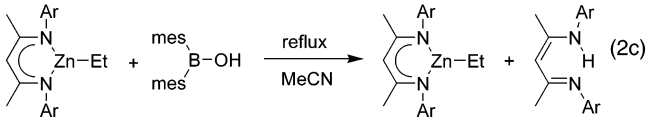

The reaction between [Zn{OB(mes)$_2$}Me]$_2$ (**2**) and neutral (BDI)H did not proceed at room temperature or in refluxing toluene, attributed to a steric conflict between the mesityl substituents of the boroxide ligand and the aryl group of the (BDI)H ligand disfavoring the

(38) Sung, M. M.; Kim, C. G.; Kim, J.; Kim, Y. *Chem. Mater.* **2002**, *14*, 826.

(39) Zechmann, C. A.; Boyle, T. J.; Rodriguez, M. A.; Kemp, R. A. *Inorg. Chim. Acta* **2001**, *319*, 137.

(40) Bourget-Merle, L.; Lappert, M. F.; Severn, J. R. *Chem. Rev.* **2002**, *102*, 3031.

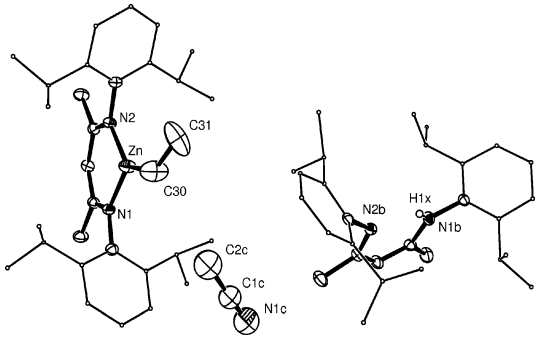

Figure 9. Unit cell contents, crystallized from MeCN, of the reaction between Zn(DBI)Et and $(mes)_2BOH$ that had been refluxed in toluene.

approach of the diketimine to the metal center. We therefore attempted the protonolysis reaction between Zn(BDI)R (R = Me, Et) and dimesitylborinic acid, in which the BDI ligand is already bonded to the metal center. As before no reaction was observed at room temperature, suggesting that steric demands of the mesityl substituents restrict the reactivity, particularly since a similar approach using smaller alcohol reagents (e.g., H_2O, MeOH, ^{i}PrOH) has previously been shown to be a viable route to $[Zn(BDI)OR]_n$ compounds.[19] Attempts at driving the reaction by using more forcing conditions (refluxing toluene) had no effect for the zinc methyl compound; however, a reaction was detected for the zinc ethyl analogue, as indicated by the loss of the $(mes)_2BOH$ resonance in the ^{1}H NMR spectrum of the crude product. An X-ray analysis of crystals obtained by crystallization from acetonitrile showed that the molecular structure consisted of the Zn(BDI)Et starting reagent that had cocrystallized with neutral (BDI)H and MeCN solvate molecule (Figure 9). This suggests that the Zn−N bond is susceptible to protonolysis by the borinic acid reagent, a result similar to that with the related zinc guanidinate system, in which the reaction between $[Zn(Me_2NC\{N^iPr\}_2)Me]_2$ and $(mes)_2BOH$ affords the mixed guanidinate-guanidine boroxide, $Zn[Me_2NC\{N^iPr\}_2][OB(mes_2)]\cdot Me_2NC\{N^iPr\}\{NH^iPr\}$.[41] The Zn(BDI)Et/(BDI)H/MeCN structure also serves to illustrate the extremely effective protection that $[BDI]^-$ offers the metal, preventing the sterically unobtrusive acetonitrile from interacting with the zinc center.

3.5. Attempted Ring-Opening Polymerization Catalysis. The initial aim of this study was to assess the merits of the Zn−BOR_2 bond in the context of lactide polymerization. Attempted preparative scale polymerizations of ϵ-caprolactone were unsuccessful using both the dimeric boroxide, $[Zn\{OB(mes)_2\}Me]_2$ (**2**), and the conventional alkoxide analogue, $[Zn\{OCH(mes)_2\}Me]_2$ (**3**). A more detailed study using NMR scale reactions with *rac*-lactide also gave a negative result for the initiation of polymerization using **2**. In contrast **3** slowly polymerized 100 equiv of *rac*-lactide under identical conditions during a 16 h period. These results suggest that, despite the predicted weakening of the zinc−oxygen bond and the removal of the steric bulk from the coordination sphere of the metal in the boroxide complexes, additional factors must be in effect that prevent the initiation and/or propagation of the polymerization reaction. Unfortunately, the numerous difficulties encountered during the synthesis of magnesium boroxide complexes prevented a similar assessment of the activity of the Mg−OBR_2 bond.

3.6. Conclusions. Two main protocols for the generation of metal boroxide complexes have been investigated in the context of zinc and magnesium chemistry: (i) protonolysis using the borinic acid and (ii) transmetalation from the lithium boroxide species. Starting from dialkyl zinc complexes, method (i) proved highly successful, with isolation of the mixed boroxide/alkyl complex in good yield. For magnesium, however, many difficulties were encountered using either (i) or (ii) as an attempted entry point. While generation of magnesium boroxide complexes has frequently been demonstrated, a high-yielding (reproducible) route failed to be developed during the course of the study. The low solubility and facile decomposition of many of these complexes contribute to the difficulties in isolating pure compounds in sufficient quantities to fully explore the chemistry.

X-ray crystallography has been extensively used in the characterization of the boroxide complexes described, indicating exclusive formation of the μ^2-coordination mode. An important contributory factor in the predilection for this ligand to bridge metal centers is believed to be the displacement of the bulky mesityl substituents away from the oxygen atom arising from the incorporation of the boron. This allows the approach of a second metal center to the oxygen and the formation of a bridging coordination mode. Investigation of the metal−oxygen bond distances indicates essentially equal distances throughout the M_2O_2 metallacycle, suggesting strongly held dimers in the solid state that are likely to maintain their structure in solution.

A brief assessment of the ROP reactivity of zinc boroxide **2** with *rac*-lactide demonstrated a total lack of catalytic behavior under the conditions investigated. Considering a coordination−insertion mechanism for the propagation step during ROP and that many of the most active systems for ROP consist of a three-coordinate metal (or a loosely held dimer that is likely to dissociate in solution), a ligand framework which allows the approach of a monomer to the metal center is essential in generating an active system. It is believed therefore that despite a predicted weakening of the metal−oxygen bond for boroxide species, the combined electron deficiency and displaced bulk associated with these ligands favors the formation of strongly held dimers that are inactive for ring-opening polymerization, and that perhaps we have gone a step too far in modifying the properties of the metal−oxygen linkage.

Acknowledgment. We thank the EPSRC for a research studentship (S.C.C.) and University of Sussex for additional financial support. We also wish to acknowledge the use of the EPSRC's Chemical Database Service at Daresbury.

Supporting Information Available: ^{1}H and ^{13}C NMR spectra of $[Mg\{OB(mes)_2\}Me(THF)]_2$ (**5**) and $[Mg\{OB(mes)_2\}^nBu(THF)]_2$ (**6**). This material is available free of charge via the Internet at http://pubs.ac.org.

OM049520J

(41) Birch, S. J.; Boss, S. R.; Cole, S. C.; Coles, M. P.; Haigh, R.; Hitchcock, P. B.; Wheatley, A. E. H. *Dalton Trans.* **2004**, in press.